DINAME 2019 - Proceedings of the XV International Symposium on Dynamic Problems of Mechanics,
M.A. Savi, T.G. Ritto and W.M. Bessa (Editors), ABCM, Buzios, RJ, Brazil, March 10th to 15th, 2019

Phenomenological models to investigate phase characteristics of plastic water pipe and ground vibration due to leak noise excitation

F.C.L. Almeida [1], M.J. Brennan [2] and O. Scussel [2]

[1] Faculty of Science and Engineering, UNESP-FCE, Rua Domingos da Costa Lopes, 780, 17602-496, Tupã-SP, Brazil

[2] Department of Mechanical Engineering, UNESP-FEIS, Avenida Brasil, 56, 15385-000, Ilha Solteira-SP, Brazil

Abstract: Old water metallic pipes have been replaced by plastic ones in many water distribution systems. This has been done to reduce water wastage due to the deterioration of metallic pipe systems. However, plastic pipes are still susceptible to leakage, and potable water, which is a scarce source, is lost, increasing the cost of water treatment and pumping, as well as affecting the environment. Acoustic techniques are widely used to detect leaks in buried pipes. They can be deployed by placing sensors on the pipe, such as using the cross-correlation technique or can be carried out by measuring the ground vibration caused by the presence of a leak, by using geophones. Reflections, wave interactions and the system dynamics, however, can jeopardize the use of such techniques. This paper investigates the use of phenomenological models based on wave theory to understand the effects that such features can cause in the measured phase. The phase gradient is related to the time delay, which is used to calculate the leak location, so that, if it is affected, then the estimation is compromised.

Keywords: Leak, Buried pipe, Wave model, Phase behaviour

INTRODUCTION

Water pipes are susceptible to leakage, which can lead to infrastructure and environmental damage. Moreover, water companies are under pressure to reduce water wastage, as this source is becoming scarce with the increase of population in large centres, together with the large distances that potable water needs to be transported. In Brazil the water loss is about 38%. However, it may reach 70% in some states, such as Maranhão (O Globo, 2018). In developed countries, such as Japan, where the water loss is about 2% (O Globo, 2018), acoustic techniques, such as the cross-correlation technique, are frequently used (Fuchs and Riehle, 1991). Another well-known technique is to measure the ground vibration using a geophone (Puust et al., 2010) “to listen” for the leak noise that propagates through the soil above the pipe.

Analytical models have been developed to gain physical insight and understanding of the mechanisms responsible for leak noise propagation in buried pipes, and pipe-soil interaction. These models are wave-based, where the wavenumber related to leak noise propagation is sought. It has been found that the wave which carries the most of leak energy in the pipe is predominantly fluid-borne (Muggleton et al., 2002). Gao et al. (2004, 2005) used this model, but neglected the soil effects to investigate the cross-correlation technique. This model was also used to investigate the effects of reflections on the time delay estimation using cross-correlation (Gao et al., 2009). When the soil is taken into account then Hankel functions are needed in the mathematical model. The most complete model was developed by Gao et al. (2017) and was approximated and rewritten by Brennan et al. (2018) in terms of water, pipe and soil stiffness to give a better physical insight and interpretation of the problem.

This paper intends to demonstrate how simple models, which are termed phenomenological models, can be used to investigate some features of the data from the more complete models, such as wave reflections and wave interaction for leak detection problems. These models are wave-based models which can be used either for leak noise propagation along the pipe and through the soil. The simple models are possible because the Hankel functions used in the complete model, tend to complex exponential functions at high frequencies (generally above 500 Hz), which is the case in this paper. Moreover, actual data is provided to show these affects in practical situations.

FULL MODEL FOR PIPE AND GROUND VIBRATION PROBLEMS

The phenomenological models, which will be used in this work to describe features that are generally found in leak detection problem, are achieved by assumptions that reduces the complexity of the wave model where the internal fluid-pipe-soil interactions are taken into account. The most complete wave model up-to-date was developed by Gao et al. (2016, 2017), and is used here to show that the assumptions made for the phenomenological models hold for the cases herein presented. This model (Gao et al., 2016, 2017) describes how the predominantly fluid-borne wave ($s=1$) (Muggleton et al., 2002) propagates along the pipe together with, the waves which radiate through the soil due to the pipe-wall displacement. The waves in the soil are shear and compressional waves. Furthermore, this wave model is

based on Hankel functions to describe the motion of the soil. Figure 1 shows a schematic diagram of the waves propagating in the pipe and radiating into the soil due to a leak excitation in a buried pipe. The parameter is the burial depth (pipe radius + soil layer above the pipe wall).

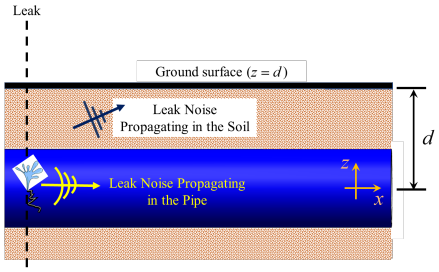

Figure 1 – Schematic of the leak noise propagating in the pipe and the soil

The normalized ground surface displacement $\tilde{U}_x$ and $\tilde{U}_z$ with respect to the radial displacement of the pipe wall W is given by (Gao et al., 2017)

$$\tilde{U}_x = \frac{\left\{\begin{array}{l}\left[k\left(1+C_{11}\right)-k_{\mathrm{r}}^{\mathrm{r}}C_{21}\right]\sqrt{\dfrac{2}{\pi k_{\mathrm{d}}^{\mathrm{r}}d}}e^{j\pi/4}\left[kH_0'(k_{\mathrm{r}}^{\mathrm{r}}a)\dfrac{1-\Omega^2-FL-SL_{22}}{j\nu_p\left(ka\right)+SL_{21}}-jk_{\mathrm{r}}^{\mathrm{r}}H_0(k_{\mathrm{r}}^{\mathrm{r}}a)\right]e^{-jk_{\mathrm{d}}^{\mathrm{r}}d}\\ +\left[k_{\mathrm{r}}^{\mathrm{r}}\left(1-C_{11}\right)+kC_{12}\right]\sqrt{\dfrac{2}{\pi k_{\mathrm{r}}^{\mathrm{r}}d}}e^{j\pi/4}\left[k_{\mathrm{d}}^{\mathrm{r}}H_0'(k_{\mathrm{d}}^{\mathrm{r}}a)\dfrac{1-\Omega^2-FL-SL_{22}}{j\nu_p\left(ka\right)+SL_{21}}+jkH_0(k_{\mathrm{d}}^{\mathrm{r}}a)\right]e^{-jk_{\mathrm{r}}^{\mathrm{r}}d}\end{array}\right\}}{k_{\mathrm{r}}^{\mathrm{r}}k_{\mathrm{d}}^{\mathrm{r}}H_0(k_{\mathrm{r}}^{\mathrm{r}}a)H_0'(k_{\mathrm{d}}^{\mathrm{r}}a)+k^2H_0'(k_{\mathrm{r}}^{\mathrm{r}}a)H_0(k_{\mathrm{d}}^{\mathrm{r}}a)} \tag{1a}$$

and

$$\tilde{U}_z = \frac{\left\{\begin{array}{l}\left[k_{\mathrm{d}}^{\mathrm{r}}\left(1-C_{11}\right)-kC_{21}\right]\sqrt{\dfrac{2}{\pi k_{\mathrm{d}}^{\mathrm{r}}d}}e^{j\pi/4}\left[kH_0'(k_{\mathrm{r}}^{\mathrm{r}}a)\dfrac{1-\Omega^2-FL-SL_{22}}{j\nu_{\mathrm{p}}\left(ka\right)+SL_{21}}-jk_{\mathrm{r}}^{\mathrm{r}}H_0(k_{\mathrm{r}}^{\mathrm{r}}a)\right]e^{-jk_{\mathrm{d}}^{\mathrm{r}}d}\\ +\left[-k\left(1+C_{11}\right)-k_{\mathrm{d}}^{\mathrm{r}}C_{12}\right]\sqrt{\dfrac{2}{\pi k_{\mathrm{r}}^{\mathrm{r}}d}}e^{j\pi/4}\left[k_{\mathrm{d}}^{\mathrm{r}}H_0'(k_{\mathrm{d}}^{\mathrm{r}}a)\dfrac{1-\Omega^2-FL-SL_{22}}{j\nu_{\mathrm{p}}\left(ka\right)+SL_{21}}+jkH_0(k_{\mathrm{d}}^{\mathrm{r}}a)\right]e^{-jk_{\mathrm{r}}^{\mathrm{r}}d}\end{array}\right\}}{k_{\mathrm{r}}^{\mathrm{r}}k_{\mathrm{d}}^{\mathrm{r}}H_0(k_{\mathrm{r}}^{\mathrm{r}}a)H_0'(k_{\mathrm{d}}^{\mathrm{r}}a)+k^2H_0'(k_{\mathrm{r}}^{\mathrm{r}}a)H_0(k_{\mathrm{d}}^{\mathrm{r}}a)}; \tag{1b}$$

where k is the complex wavenumber of the wave propagating in the pipe, $(k_{\mathrm{d}}^{\mathrm{r}})^2=k_{\mathrm{d}}^2-k^2$ and $(k_{\mathrm{r}}^{\mathrm{r}})^2=k_{\mathrm{r}}^2-k^2$ are the radial wavenumber of the shear and compressional waves, respectively; $\Omega=k_{\mathrm{L}}a$ is the non-dimensional frequency; $k_{\mathrm{L}}=\sqrt{\omega^2\rho_{\mathrm{p}}(1-\nu_{\mathrm{p}}^2)/E_{\mathrm{p}}}$ is the shell compressional wavenumber; E_{p}, ρ_{p} and ν_{p} are the Young′s modulus, density and Poisson's ratio of the pipe, respectively; $FL=\left(\rho_{\mathrm{f}}a\Omega^2J_0(k_{\mathrm{f}}^{\mathrm{r}}a)\right)\Big/\left(\rho_{\mathrm{p}}hk_{\mathrm{f}}^{\mathrm{r}}aJ_0'(k_{\mathrm{f}}^{\mathrm{r}}a)\right)$ is the fluid loading term, and

$$SL_{22}=-\mu_m\frac{\left(1-\nu_{\mathrm{p}}^2\right)}{E_{\mathrm{p}}}\frac{a}{h}\left\{2+\frac{k_{\mathrm{r}}^{\mathrm{r}}ak_{\mathrm{r}}^2a^2\left[H_0(k_{\mathrm{r}}^{\mathrm{r}}a)/H_0'(k_{\mathrm{r}}^{\mathrm{r}}a)\right]\left[H_0(k_{\mathrm{d}}^{\mathrm{r}}a)/H_0'(k_{\mathrm{d}}^{\mathrm{r}}a)\right]}{k_{\mathrm{r}}^{\mathrm{r}}ak_{\mathrm{d}}^{\mathrm{r}}a\left[H_0(k_{\mathrm{r}}^{\mathrm{r}}a)/H_0'(k_{\mathrm{r}}^{\mathrm{r}}a)\right]+k^2a^2\left[H_0(k_{\mathrm{d}}^{\mathrm{r}}a)/H_0'(k_{\mathrm{d}}^{\mathrm{r}}a)\right]}\right\}, \tag{2a}$$

and

$$SL_{21}=SL_{12}=j\mu_m\frac{\left(1-\nu_{\mathrm{p}}^2\right)}{E_{\mathrm{p}}}\frac{a}{h}ka\left\{2-\frac{k_{\mathrm{r}}^2a^2\,H_0(k_{\mathrm{d}}^{\mathrm{r}}a)/H_0'(k_{\mathrm{d}}^{\mathrm{r}}a)}{k_{\mathrm{r}}^{\mathrm{r}}ak_{\mathrm{d}}^{\mathrm{r}}a\left[H_0(k_{\mathrm{r}}^{\mathrm{r}}a)/H_0'(k_{\mathrm{r}}^{\mathrm{r}}a)\right]+k^2a^2\left[H_0(k_{\mathrm{d}}^{\mathrm{r}}a)/H_0'(k_{\mathrm{d}}^{\mathrm{r}}a)\right]}\right\}, \tag{2b}$$

are soil loading terms; ρ_{f} and B_{f} are the density and Bulk modulus of the water; $k_{\mathrm{f}}^{\mathrm{r}}=\sqrt{k_{\mathrm{f}}^2-k^2}$ is the radial wavenumber of the fluid, $k_{\mathrm{f}}=\omega/c_{\mathrm{f}}$ and $c_{\mathrm{f}}=\sqrt{B_{\mathrm{f}}/\rho_{\mathrm{f}}}$ are the fluid wave number and the free-field fluid wave-speed, respectively; $H_0(k_{\mathrm{r}}^{\mathrm{r}}a)$ and $H_0(k_{\mathrm{d}}^{\mathrm{r}}a)$ are the Hankel functions of zero order and second kind which represent the conical waves radiating through the soil from the pipe; $J_0'()=(\partial/\partial r)J_0()$; $H_0'()=(\partial/\partial r)H_0()$ and,

$$C_{11}=\frac{4k^2k_{\mathrm{d}}^{\mathrm{r}}k_{\mathrm{r}}^{\mathrm{r}}-\left[\left(k_{\mathrm{r}}^{\mathrm{r}}\right)^2-k^2\right]^2}{4k^2k_{\mathrm{d}}^{\mathrm{r}}k_{\mathrm{r}}^{\mathrm{r}}+\left[\left(k_{\mathrm{r}}^{\mathrm{r}}\right)^2-k^2\right]^2};\ C_{12}=\frac{4kk_{\mathrm{r}}^{\mathrm{r}}\left[\left(k_{\mathrm{r}}^{\mathrm{r}}\right)^2-k^2\right]}{4k^2k_{\mathrm{d}}^{\mathrm{r}}k_{\mathrm{r}}^{\mathrm{r}}+\left[\left(k_{\mathrm{r}}^{\mathrm{r}}\right)^2-k^2\right]^2};\ C_{21}=-\frac{4kk_{\mathrm{d}}^{\mathrm{r}}\left[\left(k_{\mathrm{r}}^{\mathrm{r}}\right)^2-k^2\right]}{4k^2k_{\mathrm{d}}^{\mathrm{r}}k_{\mathrm{r}}^{\mathrm{r}}+\left[\left(k_{\mathrm{r}}^{\mathrm{r}}\right)^2-k^2\right]^2}. \quad (3a,b,c)$$

The effects of reflections due to the ground surface

The model given by Eq.(1a,b) is used to show that the reflections caused by the finite media (ground surface above the pipe) has a marginal effect on the phase compared to when an infinite media (no reflection model) is considered. If the effects of the reflections are neglected, then $C_{11}=0$; $C_{12}=0$ and $C_{21}=0$. In order to carry out the simulations, the fluid, pipe and soil properties were chosen according to Brennan et al. (2018). Table 1 and table 2 show the pipe properties and, soil and water properties, respectively, used for the simulations.

Table 1 – Pipe Properties.

Properties	Values
Young's modulus, E (N/m²)	2×10^9
Density ρ (kg/m³)	900
Loss factor	0.06
Poisson's ratio	0.3
Pipe radius (mm)	35.8
Pipe-wall thickness (mm)	3.4

Table 2 – Soil and Water Properties

Properties	Soil	Water
Bulk modulus $B_{s,w}$ (N/m²)	4.5×10^9	2.25×10^9
Shear modulus, G (N/m²)	2.41×10^8	
Shear loss factor	0.15	
Density ρ (kg/m³)	2000	1000
Speed of Sound (m/s)		1500

Figures 2(a) and 2(b) show the unwrapped phases between the displacement at the pipe wall and the displacements at the ground surface considering the axial and radial directions, respectively. The black solid line and the red dotted line are related to the model with and without reflections, respectively. The phase is unwrapped up to 1400 Hz, because of numerical problems which can occur when the transcendental, which governs the wavenumber, is solved numerically. However, this is acceptable because reflections are heavily attenuated at high frequencies.

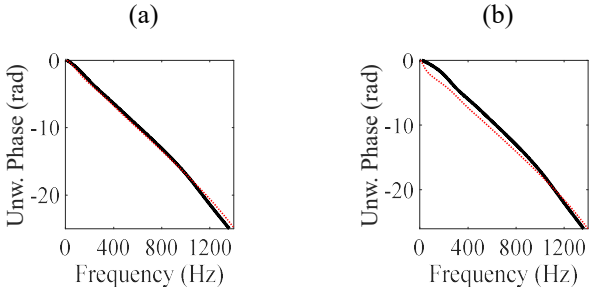

Figure 2 – The unwrapped phase considering reflection (solid black line) and no-reflected waves (dashed red line) for the Hankel function model given by Eq.(1a,b). (a) Horizontal motion. (b) Vertical motion.

It can be observed that the presence of reflections has a marginal effect on the phases. Hence, the reflections can be neglected in the model for simplicity.

Approximation of the Hankel functions with the classical plane wave model

The ground vibration model described in the previous section is based on Hankel functions which represent the wave motion due to the interaction between the pipe and soil. However, this complete model is difficult to interpret and gain physical insight. Hence, an approximate, simple model is proposed that is based on the classical plane wave model ($w_{\mathrm{p}}(x,t)$), which is used for nondispersive plane waves, and is given by

$$w_{\mathrm{p}}(l,t) = W(\omega)e^{\pm jk_{\mathrm{p}}l}e^{j\omega t}, \tag{4}$$

where $W(\omega)$ is the frequency dependent amplitude of the plane wave at the leak position, l is the distance between two measurement positions on the ground surface, $k_{\mathrm{p}} = \omega/c\,(1-j\eta/2)$ is the wavenumber (a more simplified version of k) for the plane wave, and ω, c and η are circular frequency, the speed at which the wave propagates and the loss factor, respectively. In this model, the loss factor is responsible for the wave attenuation, and the wave speed in pipes is a function of the soil properties. Furthermore, the $\pm$ sign indicates the direction of the propagating wave ("$+$" from right to left and "$-$" from left to right). Considering only the spatial dependency and a wave propagating from left to right as shown in Fig. 1, Eq. (4) can be written as $w(l)^{+} = W(\omega)e^{-jk_{\mathrm{p}}l}$. Moreover, assuming that the leak has a flat spectrum with white noise characteristics (Gao et al., 2004), so that $W(\omega) = W_0$ is constant, then Eq. (4) can be even further simplified to give

$$w(l)^{+} = W_0 e^{-jk_{\mathrm{p}}l}. \tag{5}$$

For the ground vibration problem, the Hankel functions can be asymptotically approximated by

$$w_h(r) = \mathrm{H}_0(k_{\mathrm{p}}r) \approx \sqrt{\frac{2}{\pi k_{\mathrm{p}}r}}e^{-j\left(k_{\mathrm{p}}r-\frac{\pi}{4}\right)}, \tag{6}$$

where r is the distance between the source position and the wave front. As mentioned previously, the Hankel function is responsible to describe the spherical waves that radiate from the pipe towards the soil. Eq.(5) is consistent to the theory as the intensity of the spherical wave is proportional to the inverse of the square of its radius (distance from the wave-front). Hence, Hankel can be approximated by exponential functions at higher frequencies. Knowing that two waves radiate through the soil at different wave-speeds (compressional waves-peed c_{c} and shear waves-peed c_{s}), then the wave number for each wave is a function of these parameters together with the loss factor. It is assumed that the loss factor for both waves is 0.15 (Brennan et al., 2018) and $d = 1$, for convenience. Figures 3(a) and 3(b) show the comparison between the normalized phases given by the exponential function and by the Hankel function, together with the error between them as a function of the frequency. The modified phase is calculated by removing the gradient of the phase (time delay) and shifting the phase to one radian, for convenience. For the Hankel function, the asymptote at 4 kHz is set to 1 radian. This is because ground vibration measurements can be achieved up to 4 kHz, however, the phases are shown up to 2kHz to emphasize the difference between the two models. The labels (i) and (ii) are related to the compressional (k_{c}) and shear (k_{s}) wave types, respectively. Also highlighted is the frequency at which the error between the phases is 5%.

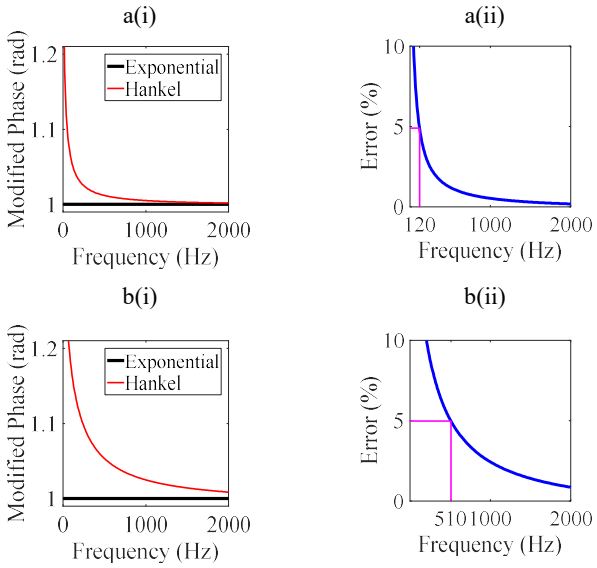

Figure 3 – The comparison between the phase given by Hankel function wave-based model and the classical plane wave-based model. (a) Normalized phase where the gradient is removed and set to unit. (b) The error between the calculated normalized phases. The labels (i) and (ii) are related to the compressional (k_c) and shear (k_s) wave types, respectively.

Observing the results given by Fig. 3 it is clear that for the shear wave the approximation is acceptable at frequencies above around 100 Hz, and for the compressional wave the approximation is valid above around 500 Hz. These "rules of thumb" are used for the phenomenological models presented in this paper when ground vibration are investigated.

ACTUAL PIPE AND GROUND VIBRATION MEASUREMENTS

Actual data collected in a special test rig is used to show that reflections can be present in leak noise signals traveling along the pipe. Moreover, ground vibration signals are also collected to show the interference between the compressional and shear waves that radiate through the soil. Figures 5(a) and 5(b) show photographs of the two test rigs for the pipe vibration signals and ground vibration signal, respectively. The test rig shown in Fig. 5(a) is located in the UK and more information can be found in Almeida et al., 2013. The test rig shown in Fig. 5(b) is located in Brazil and more information can be found in Brennan et al. (2018).

Figure 5 – Photos of the measurements. (a) The pipe vibration; (b) Ground Vibration.

Schematic diagrams showing the measurements carried out in the UK test rig and in the Brazilian test rig are shown in Figs. 6(a), and (b), respectively. For the UK test rig the leak is located 20 meters away ($b = 20$ m) from measurement position 1. The sensors are placed 30 meters ($l = 30$ m) apart and the pipe terminates with a blank. In the Brazilian pipe system, the measurements on the ground were taken at the leak position (above the leak as the pipe is underneath the ground) and the sensors are 1 meter ($l = 1$ m) apart along the pipe.

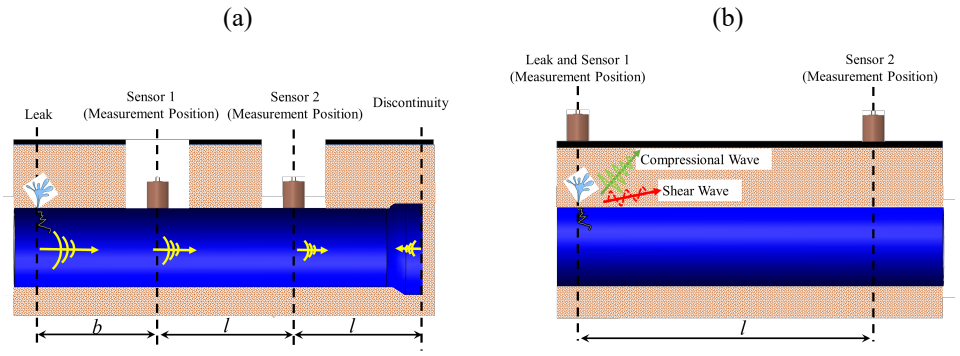

Figure 6 – Schematic of the problems investigated. (a) Reflection; (b) Interaction between two waves.

The coherence, modulus of the CPSD (|CPSD|) and unwrapped phase of the CPSD are shown in Figure 7(a), 7(b) and 7(c), respectively. The labels (i) and (ii) are related to measurements on the pipe and the soil vibration, respectively. It is observed that (specially at the unwrapped phase) when reflections are present in the pipe (Fig. 7c(i)), wobbles and additional phase shifts are present in the actual data. Moreover, the phase has a straight-line behavior, which is related the non-dispersive characteristic of the leak noise propagation in the pipe. On the other hand, for the case of ground vibration, two different phase gradients are evident. These phase gradients are related to the two waves (shear and compressional waves) that propagate between the two sensors, but dominate at different frequency ranges. Hence, measurement on the pipe and on the ground along the pipe have different characteristics, which are further investigated here.

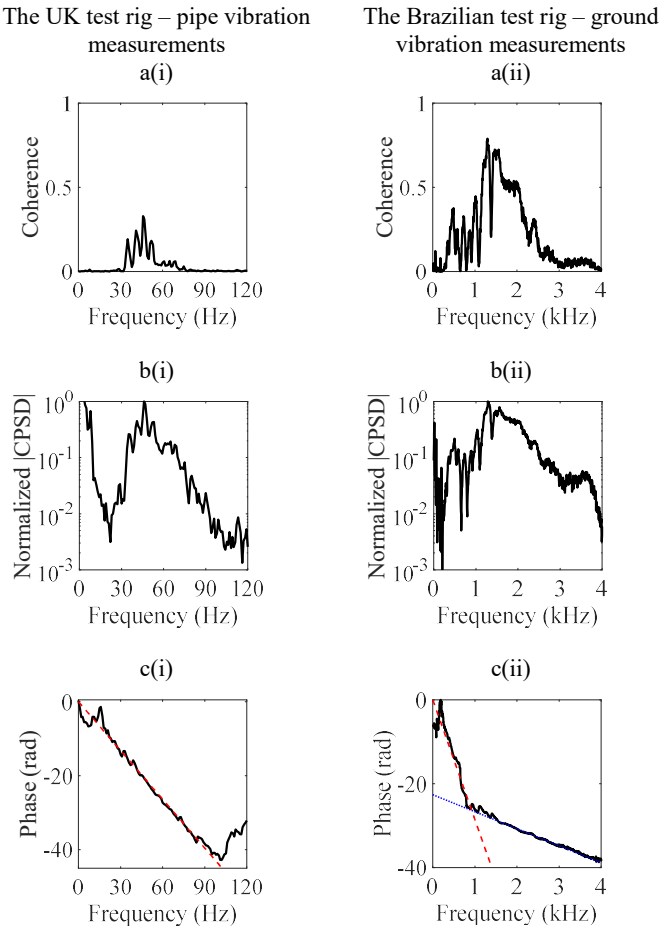

Figure 7 – Measured data. (a) Coherence; (b) Modulus of the CPSD. (c) Unwrapped phase. The labels "i" and "ii" are related to the pipe measurements and ground vibration measurements, respectively. Measured data (black-solid line); Estimated gradient for the compressional wave (red-dashed line); Estimated gradient for the shear wave (blue-dotted line).

The phase characteristic in Figure 7(c) is due to the mechanisms that the leak excitation propagates through the soil. In the Brazilian test rig the shear wave is due to the leak (source), while that, the compressional wave is radiated by the pipe. Hence, it is clear from the measurements shown in Fig. 7 that the vibration along the pipe due to the leak has different characteristics that the vibration measured above the pipe (on the ground).

To interpret the data presented in the previous section, phenomenological models are used. The interaction between the two waves, as shown in Fig. 6(b) when shear and compresstional waves, which wavenumbers are k_s and k_c, respectively, propagate in the soil can be modelled as

$$w(l) = W_0^s e^{-jk_s l} + W_0^c e^{-jk_c l}, \tag{7}$$

where W_0^c and W_0^s are the frequency dependant amplitudes of the longitunal and shear wave, respectively, but here are considering costant for simplicity, and l is the distance from the leak to the measurement position, which here is assumed to be 1 meter. The Cross Power Spectral Density (CPSD) Function, for this case, can be calculated as

$$S_{12}(\omega) = S_0\, w(l)/w(0). \tag{8}$$

The CPSD is used in practical situations to measure the phase in leak problems. It is also assumed that $c_s = 220$ m/s, $c_c = 1550$ m/s and $\eta_s = \eta_c = 0.15$. Figure 8(a) and 8(b) show the normalized modulus $S_{12}(\omega)/S_0$ and the phase for simulations using Eq.(8) (solid-black line). The ratio $R = W_0^c/W_0^s$ is set at 0.2. The amplitudes of the shear (red-dashed line) and longitudinal (blue-dotted line) waves intersect at around 900 Hz. Hence, the phase is dominated by the shear wave (see Fig. 8(b)) below such frequency (it fluctuates around the phase due to the shear wave) and by the longitudinal wave above such frequency (the phase fluctuates at the flat trend as for the longitudinal wave). Moreover, there is an additional phase shift at the frequency where the two amplitudes intersect. Figure 9(c) shows the predicted phase (red solid thin line) by using Eq.(8) overlaying the actual phase (solid black thick line), which is the same shown in Fig. 7c(ii). As the predicted phase was carried out above 100Hz for the shear wave and above the 900Hz for the compressional wave, the "rule of thumb" for the approximation of Hankel functions by exponential ones mentioned previously hold and the phenomenological model can be used.

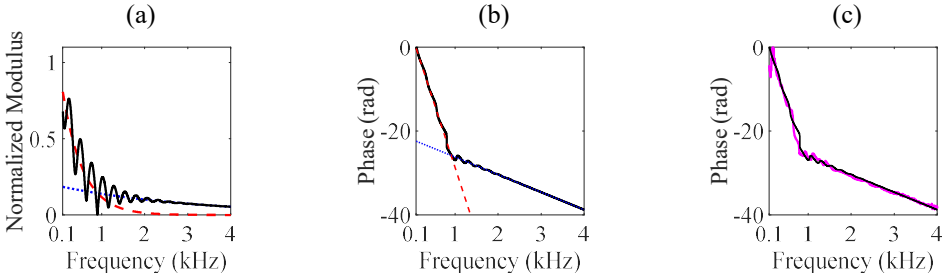

Figure 8 – The results calculated using Eq.(8) (Black-solid line). (a) $S_{12}(\omega)/S_0$; (b) Phase. The components of the Shear wave (red-dashed line) and Longitudinal wave (blue-dotted line) are also shown for convenience; (c) Comparison between the actual phase (solid thick magenta line) and simulated phase (Black-solid line).

CONCLUSION

This paper has shown two different phenomenological wave-based models which can be used to investigate general problems found when using acoustic techniques to detect leaks. These are reflections and the interaction between two waves propagating in the soil. They were validated by using complex models based on Henkel Functions that connect the effects of the fluid-born wave couples between the fluid and the pipe-wall together with the soil interaction. The first can be noticed by fluctuations in the modulus and phase of measured data. The second can be observed as fluctuations in the modulus and phase together with two additional phase shifts and slopes when the amplitudes of the two propagating waves are at the same level at a certain frequency. Actual leak data measured in the pipe and in the soil were also used to support the results herein discussed.

ACKNOWLEDGMENTS

The authors would like to thank the financial support provided by the São Paulo Research Foundation (FAPESP) under Grant numbers 2013/50412-3 and 2017/14432-0.

REFERENCES

Almeida, F. Improved acoustic methods for leak detection in buried plastic water distribution pipes. 2013, 274 p. Phd Thesis - University of Southampton, Southampton.

Brennan, M.J., Karimi, M., Muggleton, J.M., Almeida, F.C.L., Lima, F.K., Ayala, P.C., Obata, D., Paschoalini, A.T. and Kessissoglou, N., 2018, "On the effects of soil properties on leak noise propagation in plastic water distribution pipes", Journal of Sound and Vibration, Vol. 427, pp. 120-193.

Fuchs, H.V., and Riehle, R., 1991, "Ten years of experience with leak detection by acoustic signal analysis", Applied Acoustic, Vol. 33, pp. 1-19.

Gao, Y., Brennan, M.J., Muggleton, J.M. and Hunaidi, O., 2004, "A model of the correlation function of leak noise in buried plastic pipes", Journal of Sound and Vibration, Vol. 277, pp. 133-148.

Gao, Y., Brennan, M.J., Joseph, P.F., Muggleton, J., Hunaidi, O., 2005, "On the selection of acoustic/vibration sensors for leak detection in plastic water pipes", Journal of Sound and Vibration, v. 283, p. 927-941.

Gao, Y., Brennan, M.J., and Joseph, P.F., 2009, "On the effects of reflections on time delay estimation for leak detection in buried plastic water pipes", Journal of Sound and Vibration, Vol. 325, pp.649-663.

Gao Y., Sui F., Muggleton J.M, Yang J., 2016, Simplified dispersion relationships for fluid-dominated axisymmetric wave motion in buried fluid-filled pipes, Journal of Sound and Vibration, vol. 375, pp. 386–402.

Gao, Y., Brennan, M.J., Muggleton, J.M., Liu, Y., and Rustighi, E., 2017, "An analytical model of ground surface vibration due to axisymmetric wave motion in buried fluid-filled pipes", Journal of Sound and Vibration, Vol. 395, pp. 142-159.

Muggleton, J.M., Brennan, M.J., and Pinnington, R.J., 2002, "Wavenumber prediction of waves in buried pipes for water leak detection", Journal of Sound and Vibration, Vol. 249, No. 5, pp. 939-954.

O Globo, 24th of March 2018, printed version.

Puust, R., Kapelan, Z., Savic, D.A., and Koppel, T., 2010, "A review of methods for leakage management in pipe networks", Urban Water Journal, Vol. 7, No. 1, pp. 25-45.

RESPONSIBILITY NOTICE

The authors are the only responsible for the printed material included in this paper.